Journal of Ethnopharmacology xxx (xxxx) xxx

Contents lists available at ScienceDirect

Journal of Ethnopharmacology

journal homepage: www.elsevier.com/locate/jethpharm

Kaempferol attenuates streptozotocin-induced diabetic nephropathy by downregulating TRAF6 expression: The role of TRAF6 in diabetic nephropathy

Wu Luo [a,1], Xiaojun Chen [a,e,1], Lin Ye [a,1], Xuemei Chen [a,1], Wenjing Jia [a], Yanni Zhao [a], Aleksandr V. Samorodov [b], Yali Zhang [a], Xueting Hu [a], Fei Zhuang [a,c], Jianchang Qian [a,d], Chao Zheng [a,c], Guang Liang [a,d,**], Yi Wang [a,d,*]

[a] Chemical Biology Research Center, School of Pharmaceutical Sciences, Wenzhou Medical University, Wenzhou, 325035, China
[b] Department of Pharmacology, Bashkir State Medical University, Ufa City, 450005, Russia
[c] Department of Endocrinology, The Second Affiliated Hospital and Yuying Children's Hospital of Wenzhou Medical University, Wenzhou, Zhejiang, 323000, China
[d] Zhuji Biomedicine Institute, School of Pharmaceutical Sciences, Wenzhou Medical University, Zhuji, Zhejiang, 311800, China
[e] Laboratory of Pharmaceutical Analysis, Department of Pharmaceutics, Wenzhou Nursing School, Wenzhou, Zhejiang, 325000, China

ARTICLE INFO

Keywords:
Kaempferol
Diabetic nephropathy
Inflammation
TRAF6
Renal tubular epithelial cells

ABSTRACT

Ethnopharmacological relevance: Kaempferia rhizome is a famous traditional herbal medical in tropical and subtropical areas. Kaempferol (KPF) is one of the main bioactive compounds in Kaempferia rhizome, with antioxidant/anti-inflammatory effects demonstrated in various disease models, including cancers, obesity and diabetes.

Aim of the study: Inflammation plays an important role in the pathogenesis of diabetic nephropathy (DN). TRAF6 functions as a signal transducer in toll-like receptor 4 and NF-κB pro-inflammatory signaling pathway. We aimed at investigate whether KPF is able to mitigate inflammatory responses by regulating TRAF6 in DN.

Material and methods: C57BL/6 mice were injected with streptozotocin to induce type 1 DN. NRK-52E, a tubular epithelial cell line, was used for *in vitro* analysis. TRAF6 was knockdown using siRNA *in vitro* and AAV2/2-shRNA *in vivo*. The anti-DN and inflammatory effects of KPF or knockdown of TRAF6 were evaluated by investigating renal filtration index, pathological changes of kidney tissue. Proinflammatory cytokine levels were detected using ELISA. NF-κB pathway and protein levels of related pathways were detected through Western blot.

Results: KPF significantly reduced renal inflammation, fibrosis, and kidney dysfunction in diabetic mice. These effects were associated with a downregulation of TRAF6 in diabetic mouse kidneys, indicating the potential role of TRAF6. Knockdown of TRAF6 in mice through AAV2-shTRAF6 confirmed the importance of TRAF6 in DN. *In vitro*, treatment of KPF in NRK-52E cells attenuated high glucose (HG)-induced inflammatory and fibrogenic responses, associated with downregulated TRAF6 expression. The conclusion was further confirmed in NRK-52E cells by knocking down the expression and by overexpression of TRAF6.

Conclusion: Our findings provide direct evidence that TRAF6 mediates diabetes-induced inflammation leading to renal dysfunction. We also show that KPF is a potential therapeutic agent to reduce inflammatory responses in DN. Also, TRAF6 may represent an interesting target to combat DN.

* Corresponding author. Chemical Biology Research Center, School of Pharmaceutical Sciences, Wenzhou Medical University, Wenzhou 325035, China.
** Corresponding author. Chemical Biology Research Center, School of Pharmaceutical Sciences, Wenzhou Medical University, Wenzhou, 325035, China.
E-mail addresses: hat890316@hotmail.com (W. Luo), 495594859@qq.com (X. Chen), 982571711@qq.com (L. Ye), 120359331@qq.com (X. Chen), 15067897058@163.com (W. Jia), 1021087849@qq.com (Y. Zhao), avsamorodov@gmail.com (A.V. Samorodov), ya-li000@163.com (Y. Zhang), rosefloor@163.com (X. Hu), 1165194084@qq.com (F. Zhuang), qianjc@wmu.edu.cn (J. Qian), wallbb_1022@163.com (C. Zheng), wzmaliangguang@163.com (G. Liang), yi.wang1122@wmu.edu.cn (Y. Wang).
[1] These authors contributed equally to this work.

https://doi.org/10.1016/j.jep.2020.113553
Received 13 June 2020; Received in revised form 26 October 2020; Accepted 30 October 2020
Available online 3 November 2020

Abbreviations

AAV2/2	adeno-associated virus type 2/mutant 2
AMPK	AMP-activated protein kinase
AQP1	aquaporin 1
BUN	blood urea nitrogen
Col-IV	Collagen IV
DN	diabetic nephropathy
ECM	extracellular matrix
H&E	hematoxylin and eosin
HG	high-concentration glucose
IHC	immunohistochemistry
IKK	inhibitor of κB kinase
IL-6	interleukin-6
IRAK	interleukin-1 receptor-associated kinase
JNK	c-Jun N-terminal kinase
KPF	kaempferol
MAPK	mitogen-activated protein kinase
mTOR	mechanistic target of rapamycin
MyD88	myeloid differentiation primary response protein
NF-κB	nuclear factor-κB
PBS	phosphate-buffered saline;
PCR	polymerase chain reaction
qPCR	quantitative PCR
STZ	streptozotocin
T1DM	type 1 diabetes
TAK1	TGF-β activated kinase-1
TGF-β	transforming growth factor-β;
TLR-4	Toll-like receptors-4
TNF-α	tumor necrosis factor- α;
TRAF6	tumor necrosis factor receptor associated factor 6
WT-1	Wilms tumor 1

1. Introduction

Diabetic nephropathy (DN) is one of the most prominent and clinically challenging microvascular complications of diabetes and end-stage renal disease worldwide. One-third of all patients with type 1 diabetes (T1DM) develop DN (Gheith et al., 2016). Structural and cellular changes in DN include glomerular hypertrophy, hyperfiltration, glomeruli and tubulointerstitial inflammation, and extracellular matrix (ECM) protein accumulation (Gheith et al., 2016). Chronic hyperglycemia creates a milieu of inflammation through stimulating renal cells and infiltrating macrophages that drives the progression of DN (Aghadavod et al., 2016). A recent study has also indicated that hyperglycemia activates innate immunity, which may be the main driving factor for the inflammation in the kidneys (Lim and Tesch, 2012).

Toll-like receptor 4 (TLR4), a pattern-recognition receptor for lipopolysaccharide, is the most characterized member of the TLR family in innate immunity (Reynolds et al., 2012). Upon binding of ligands to TLR4, the essential adaptor myeloid differentiation primary response protein (MyD88) is recruited to TLR4 as a dimmer. MyD88 then recruits interleukin-1 receptor-associated kinase (IRAK), activating downstream signaling pathway including IRAK-1, IRAK-4, and then tumor necrosis factor receptor-associated factor 6 (TRAF6). IRAK-1, in association with TRAF6, triggers the activation of mitogen-activated protein kinases (MAPK) and inhibitor of κB (IκB) kinase (IKK) complex. Subsequently, phosphorylation of IκB by IKK causes IκB degradation that liberates nuclear factor-κB (NF-κB) (Akira and Takeda, 2004). Translocation of NF-κB to the nucleus induces the expression of target genes which include tumor necrosis factor (TNF)-α, interleukin 6 (IL-6), and other inflammatory cytokines.

Studies have shown that overactivation of the TLR4-MyD88-NF-κB signaling axis by hyperglycemia induces inflammation and tubulointerstitial fibrosis and drives the progression of nephropathy in diabetic mice (Liu et al., 2014; Ma et al., 2014). TLR4 deficiency has also been shown to be protective against renal inflammation, fibrosis, and podocytopathy in diabetic mice (Jialal et al., 2014; Ma et al., 2014). Studies have also reported increased TLR4 expression and activity induced by high levels of glucose in mesangial cells (Kaur et al., 2012), podocytes (Ma et al., 2014) and tubular epithelial cells (Liu et al., 2014; Ma et al., 2014). Treatment of diabetic mice with ellagic acid, a natural phenol antioxidant, protected against kidney dysfunction by inhibiting TLR4-NF-κB (Zhou et al., 2019). These studies underscore the importance of TLR4-NF-κB pathways in the pathogenesis of DN. Interestingly, expression of TRAF6 has also been found to be elevated in diabetic patients (Lenin et al., 2015) and implicated in the progression of DN (Zhou et al., 2019).

Natural compounds and their derivatives have been tested for various diseases, including cancer, and diabetes (Al-Dabbagh et al., 2018, 2019; Hamza et al., 2018). Kaempferia galanga L., is a stemless, rhizomatous, aromatic, perennial and indigenous herb. a widely consumed and valuable medicinal and edible plant belonging to the family of Zingiberaceae in most tropical and subtropical areas. It has been reported to have multiple biological activities including anti-inflammation, anti-tuberculosis, anti-dengue, anti-nociceptive, anti-angiogenic, anticancer, anti-hyperlipidemic, sedative, vasorelaxant and wound healing (Jagadish et al., 2016; Kumar, 2020).

Kaempferol (KPF, chemical structure shown in Fig. 1A, is one of the major bioactive compounds extracted from the rhizome of K. galanga. KPF has been shown to exhibit a range of pharmacological properties against oxidative stress (Liao et al., 2016), cancers (Kim et al., 2018), inflammatory conditions (O et al., 2015), obesity (Zang et al., 2015), and diabetes (Alkhalidy et al., 2018; Luo et al., 2015). Recently, we have shown that KPF attenuated hyperglycemia-induced cardiac injury by inhibiting NF-κB (Chen et al., 2018a). Although the direct molecular targets of KPF are not known, studies have indicated modulation of MAPK pathway in diabetic retinopathy and cardioprotection (Feng et al., 2017; Xu et al., 2017), and AMP-activated protein kinase (AMPK)/mechanistic target of rapamycin (mTOR) in cytoprotection (Varshney et al., 2017).

In this study, we investigated potential activity of KPF against inflammatory responses in DN. Using the streptozotocin-induced diabetic mouse model, we showed that KPF attenuated inflammatory responses in kidneys and protected against kidney dysfunction. We found that these activities were mediated, at least in part, through modulating TRAF6. We then confirmed the significant contribution of TRAF6 in tubular epithelial cells challenged with high glucose levels.

2. Materials and methods

2.1. Reagents and chemicals

Kaempferol was obtained from Sigma-Aldrich (St. Louis, MO, USA) and was dissolved in dimethyl sulfoxide (DMSO) for *in vitro* studies and 1% sodium carboxymethyl cellulose (CMC-Na) for *in vivo* studies. Antibodies against NF-κB p65 subunit (cat.no. sc-8008), inhibitor of nuclear factor kappa B subunit alpha (IκB-α, cat. no. sc-1643), phosphorylated (p) (cat.no. sc-6254) and total Jun N-terminal kinase (JNK) (cat.no. sc-137019) and TGF-β activated kinase-1 (TAK1) (cat.no. sc-7967), Lamin B (cat.no. sc-374015), and Glyceraldehyde-3-Phosphate Dehydrogenase (GAPDH) (cat.no. sc-32233)were obtained from Santa Cruz Biotechnology (Dallas, Texas, USA). Antibodies against TNF-α (cat.no. ab1793), TLR4(cat.no. ab22048), MyD88(cat.no. ab 2064), TRAF-6(cat.no. ab33915), transforming growth factor-β (TGF-β)

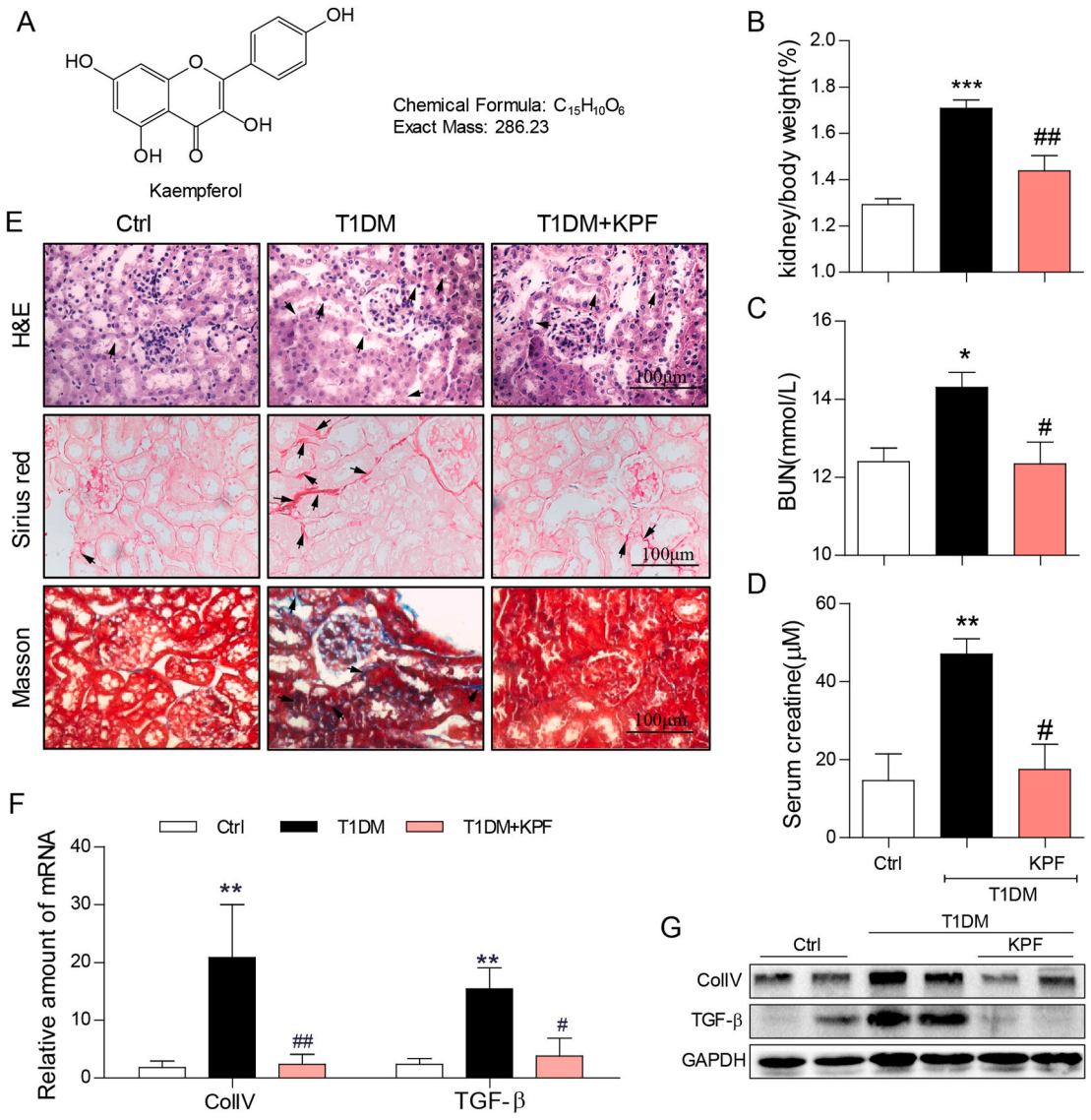

Fig. 1. Kaempferol normalizes diabetes-induced renal dysfunction and tissue fibrosis. (A) Chemical structure of Kaempferol. **(B)** Assessment of kidney to body weight ratios. **(C–D)** Levels of blood urea nitrogen (BUN) and serum creatinine (Cr) in diabetic mice and mice treated with KPF. **(E)** Representative images for H&E, Sirius red and Masson Trichome staining [scale bar = 100 μm]. **(F)** mRNA levels of Col-IV and TGF-β in kidney tissues of mice as determined by qPCR [mRNA levels were normalized to β-actin]. **(G)** Western blot analysis of Col-IV, and TGF-β levels in kidney samples from nondiabetic and diabetic mice, and diabetic mice treated with KPF. Data are presented as mean ± SEM (n = 8; *p < 0.01 compared to non-diabetic control; #p < 0.05 compared to T1DM). (For interpretation of the references to colour in this figure legend, the reader is referred to the Web version of this article.)

(cat.no. ab92486), Collagen IV (cat.no. ab6586), were obtained from Abcam (Cambridge, MA, USA). Horseradish peroxidase-conjugated secondary antibodies: goat anti-rabbit IgG-HRP (cat.no. sc-2004) and goat anti-mouse IgG-HRP (cat.no. sc-2005) were from Santa Cruz Biotechnology (Dallas, Texas, USA). Mouse IL-6 and TNF-α uncoated ELISA Kit (cat.no. 88-7066-88 and cat. no. 88-7324-88) and high binding 96 well plates (cat.no. 3855) were obtained from Invitrogen (Grand Island, NY, USA).

2.2. Cell culture studies

Human embryonic kidney (HEK) 293T cells (cat.no. SCSP-502) and rat tubular epithelial cells NRK-52E (cat.no. GNR 8) were obtained from the Shanghai Institute of Biochemistry and Cell Biology (Shanghai, China). NRK-52E cells were grown in DMEM (cat.no. 10567022), containing 5.5 mM D-glucose, 5% fetal bovine serum (FBS), 100 U/mL of penicillin, and 100 mg/mL of streptomycin. Cells were challenged with DMEM medium containing 33 mM of glucose in the high glucose groups (HG). HEK-293T cells were cultured in DMEM (cat.no. 10567022), supplemented with 5.5 mM of glucose, 10% FBS, 100 U/mL penicillin, and 100 U/mL streptomycin. All regents of cell culture were obtained from Gibco (Eggenstein, Germany).

HEK-293T and NRK-52E cells were transfected with pXC-TRAF6 plasmid (gifts from Xia Lab, Life Science Institute, Zhejiang University) using Lipofectamine® 3000 (cat. no. L3000015, Invitrogen, Carlsbad, CA). Transfected cells were then exposed to HG for *in vitro* studies. To silence TRAF6, we used siRNA from Gene Pharma Co. (Shanghai, China). Specific siRNA sequence for Rat TRAF6 was 5′-AGGAGACAGGUUUCUUGUGdTdT-3’. Transfections were carried out using Lipofectamine® 3000 (Invitrogen, Carlsbad, CA).

2.3. Animal experiments

All animal care and experimental procedures were approved by the Wenzhou Medical University Animal Policy and Welfare Committee, and all animals received humane care according to the National

Institutes of Health guidelines (USA). 4–5 weeks male C57BL/6 mice (totally n = 56) were obtained from Beijing Vital River Laboratory Animal Technology Co., Ltd. (Beijing, China) and maintained in the specific pathogen-free facility at Animal Centre of Wenzhou Medical University (Wenzhou, China). All animal models were kept on constant room temperature (25 °C) with a 12/12h light/dark cycle and fed with sterile water and a standard rodent diet (Cat. no. #MD12031, MediScience Diets Co. LTD, Yangzhou, China). . 6–7 weeks male C57BL/6 mice were performed and analyzed through blinded experimenters. Mice and cage were randomly divided into each group.

To induce type 1 diabetes, C57BL/6 male mice were injected intraperitoneally with single dose of streptozotocin (180 mg/kg in 0.1 M citrate buffer, pH 4.5), while the control animals were received the same volume of citrate buffer. The fasting-blood glucose level was measured using glucometer after 4–6 h of fasting. One week after STZ injection, diabetic mice were defined as fasting-blood glucose >216 mg/dL. The diabetic nephropathy was developed 4 months after STZ-induced hyperglycemia.

1) For KPF treatment, 24 C57BL/6 mice were randomly divided into 3 groups (n = 8 per group). Two weeks after STZ injection, diabetic mice were randomly divided into 2 groups: T1DM (n = 8) and KPF-treated T1DM (T1DM + KPF, n = 8). In the T1DM + KPF group, KPF (10 mg/kg dissolved in 1% CMC-Na) was administered through oral gavage daily. The dose of KPF is based on our previous study in diabetic mice showing cardioprotective effects (Chen et al., 2018a). The T1DM group and negative control group (n = 8) received the same volume of 1% CMC-Na solution daily. Bodyweight and fasting-blood glucose levels were measured weekly. Fourteen weeks after treatment, mice were killed under sodium pentobarbital (i.p., 100 mg/kg) anesthesia.

2) For TRAF6 knockdown, adeno-associated virus type/mutant 2 (AAV2) has been reported to produce robust expression in renal tissue (Qi et al., 2013). shRNA targeting TRAF6-AAV2/2-U6-TRAF6 (titer 2.6×10^{12} GC/mL) and negative control AAV2/2-U6-NC (titer 6.4×10^{12} GC/mL) from Genechem (Shanghai, China) were used. The shRNA sequence targeting TRAF6 was 5′-aattcgCAGGTATCTTGAGAAGCCAATGGAA ttcaagagaTTCCATTGGCTTCTCAAGATACCTGttttttg-3'; The negative control short hairpin RNA sequence was 5′-aattcgTTCTCCGAACGTGTCACGTAAttcaagagaT TACGTGACACG TTCGGAGAAttttttg-3'. C57BL/6 mice (n = 16) were injected via tail vein with 1×10^{11} GC AAV2/2 expressing TARF6 shRNA (AAV2/2 shTARF6) one week before STZ injection. The negative control groups (n = 16) were injected the same titer of AAV2 expressing negative control sequence (AAV2/2-NC). One half of mice in AAV2/2 shTARF6 or negative control group received single intraperitoneal injection of STZ (180 mg/kg in 0.1 M citrate buffer, pH 4.5) and the other group received an equal volume of vehicle daily. Two weeks after STZ injection, all STZ-injected mice were considered as diabetic (fasting-blood glucose >12 mM), resulting in 4 treatment groups in total: (i) AAV2/2-NC-treated control mice that received phosphate buffered saline (PBS) (AAV2-NC group, n = 8); (ii) AAV2/2-NC-treated mice with STZ (AAV2/2-NC + T1DM group, n = 8); (iii) AAV2/2 shTARF6-treated mice that received PBS (AAV2/2 shTARF6, n = 8); (iv) AAV2/2 shTARF6-treated mice with STZ (AAV2/2 shTARF6+T1DM, n = 8). After STZ injection, these four groups were normally fed for 16 weeks to develop diabetic nephropathy.

At the indicated time points, animals were killed under sodium pentobarbital anesthesia (i.p. injection of 0.2 mL sodium pentobarbital at 100 mg mL^{-1}). Blood and renal tissues were collected at the time of sacrifice. Body weight and right kidney weight were recorded. The collected blood samples were centrifuged at 4 °C at 3000 rpm for 10 min to collect serum. Serum creatinine, urinary albumin, and urinary creatinine were detected using commercial kits (Nanjing Jiancheng Co., Jiangsu, China). Kidney tissues were either fixed in 4% paraformaldehyde for histological analysis or flash-frozen in liquid nitrogen for gene and protein expression studies.

2.4. Real-time quantitative PCR

Total RNA from cells and kidney tissues were extracted using TRIZOL (Invitrogen, Carlsbad, CA). Reverse transcription and quantitative PCR (RT-qPCR) were performed using M-MLV Platinum RT-qPCR Kit (Invitrogen, Carlsbad, CA). Real-time qPCR was carried out using the Eppendorf Real plex 4 instruments (Eppendorf, Hamburg, Germany). Primers for genes including TNF-α, IL-6, collagen IV, TGF-β, TRAF6, and β-actin were synthesized and obtained from Invitrogen (Invitrogen, Shanghai, China). The primer sequences used are provided in the supplementary Table S1. The relative amount of each gene was detected and normalized to the amount of β-actin.

2.5. Western blotting

Lysates from cells and homogenized kidney tissues were separated through 10% sodium dodecyl sulfate-polyacrylamide gel electrophoresis (SDS-PAGE) and electro-transferred to a polyvinylidene fluoride membrane (Bio-Rad Laboratory, Hercules, CA). Each membrane was pre-incubated in blocking buffer (5% non-fat milk in tris-buffered saline containing 0.05% Tween 20, TBS-T) for 1.5 h at room temperature. Membranes were then incubated with specific primary antibodies. Immunoreactive bands were detected by incubating with secondary antibodies conjugated with horseradish peroxidase for 1–2 h at room temperature and visualized with enhanced chemiluminescence reagent (Bio-Rad, Hercules, CA, USA).

2.6. Tissue staining

Kidney tissues from mice were fixed in 4% paraformaldehyde and embedded in paraffin. Tissues were then cut into 5-μm thick sections and stained with hematoxylin and eosin (H&E) for histology and Masson Trichrome and Sirius Red staining to assess fibrosis. Stained sections were viewed under microscope (Nikon, Japan).

For immunohistochemistry, 5-μm thick sections were dewaxed and hydrated in graded alcohol series. After antigen retrieval and blocking with 5% serum albumin, the sections were incubated with anti-TNF-α antibody (abcam, cat. no. ab6671, 1:200) overnight at 4 °C followed by PE-labeled mouse anti rabbit secondary antibody (Santa Cruz Biotechnology; cat. no. sc-3753, 1:500) for 1 h at room temperature. DAPI was used for counterstaining. For double labeling, sections were incubated with both TRAF6 antibody (Abcam, ab207321, 1:200) and an antibody against Wilms tumor 1 (Novus Biologicals, Littleton, CO; NBP2-44,607, 1:200) or aquaporin 1 (Santa Cruz Biotechnology; sc-32737, 1:200). Slides were then incubated with 2 secondary antibodies (TRITC-labeled secondary, Abcam, ab6786, 1:500 or Alexa Fluor488–labeled secondary, Abcam, ab150077, 1:500) for 1 h at room temperature.

2.7. Statistical analysis

All experiments were randomized and blinded. In all *in vitro* experiments, data represented 5 independent experiments and expressed as means ± SEM. Statistical analysis was performed using GraphPad Prism 6.0 software (San Diego, CA, USA). One-way ANOVA followed by Dunnett's post hoc test was used when comparing more than two groups of data. One-way ANOVA (non-parametric Kruskal–Wallis test), followed by Dunn's post hoc test was used when comparing multiple independent groups. *P* values of ˂ 0.05 were considered to be statistically significant. Post-tests were run only if F achieved $P < 0.05$ and there was no significant variance in homogeneity.

3. Results

3.1. Kaempferol protects against diabetes-induced renal fibrosis and dysfunction

We first investigated the renoprotective effects of KPF in streptozotocin (STZ)-induced diabetic mouse model by treating mice with 10 mg/kg KPF. Hyperglycemia was accompanied by significant decreases in body weight gain in diabetic mice compared to control mice, while treatment with KPF reduced blood glucose levels and partially restored body weight gain in diabetic mice (Supplementary Fig.S1). Diabetic mice also showed increased kidney to body weight ratios, and blood urea nitrogen (BUN) and serum creatinine (Cr) levels (Fig. 1B-D, respectively). These changes were not observed in diabetic mice treated with KPF indicating that KPF protected kidney function in diabetes (Fig. 1B–D).

We next analyzed the effects of KPF on kidney tissues through histological assay. Structural hallmarks of advanced DN include tubulointerstitial injuries with excessive ECM protein deposition in the glomeruli and tubulo-interstitium (Liu et al., 2014; Ma et al., 2014) and basement membrane thickening (Zhou et al., 2019). H&E staining of kidney tissues from diabetic mice showed atypical tubular epithelia,

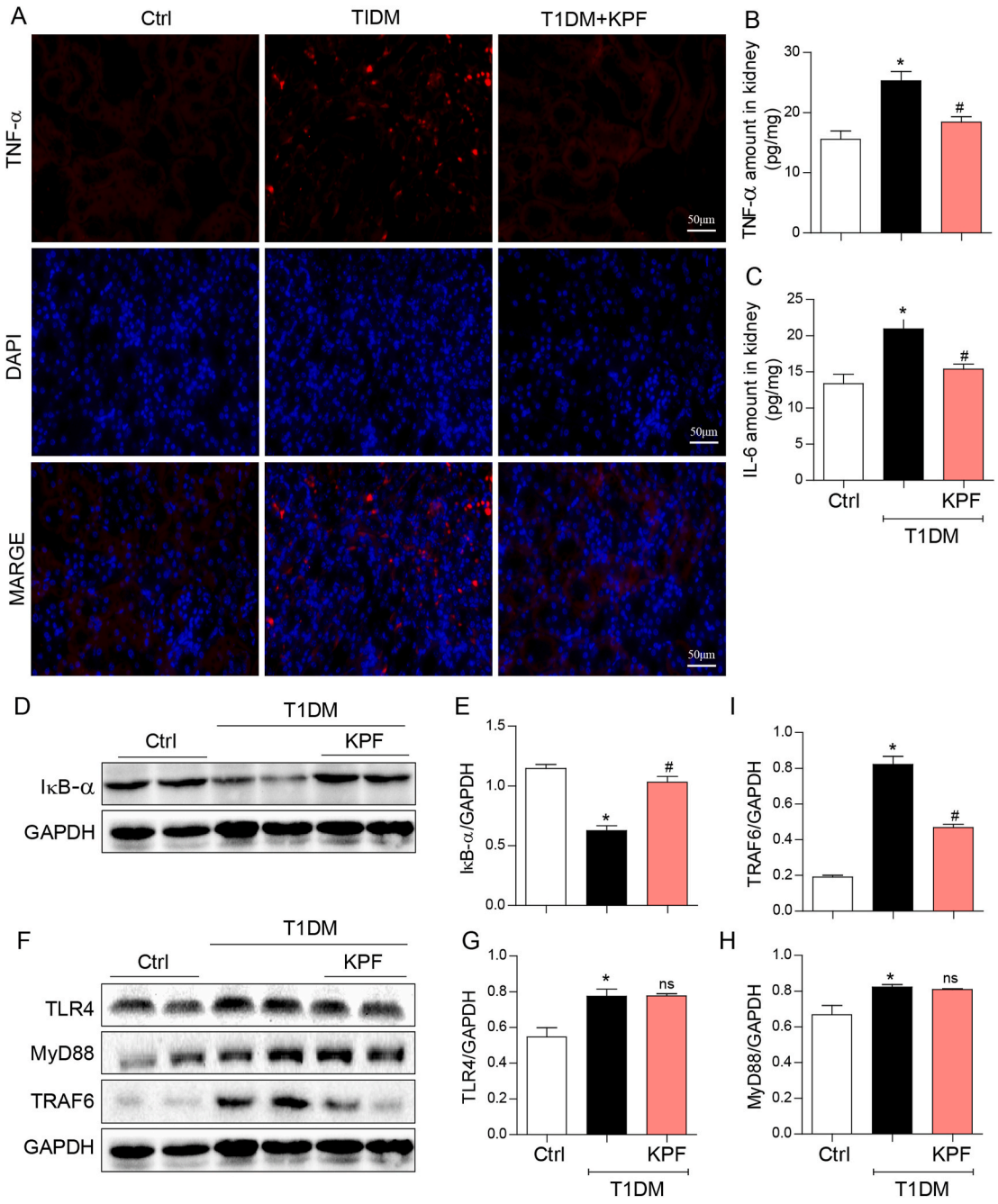

Fig. 2. Kaempferol reduces diabetes-induced inflammatory factor levels in kidneys by inhibiting NF-κB. (A) Representative images of TNF-α immunoreactivity in kidney tissues [scale bar = 50 μm]. Levels of TNF-α **(B)** and IL-6 **(C)** proteins in kidney tissues as detected by ELISA (n = 6–8). **(D)** Western blot analysis of IκB-α in kidney tissue. IκB-α levels were used as surrogate for NF-κB activity. **(E)** Densitometric analysis of IκB-α levels [representative blots are shown in panel D]. **(F)** Western blot analysis of TLR4 and TLR4 pathway proteins MyD88 and TRAF6 in kidney tissues. **(G–I)** Densitometric analysis of TLR4 pathway proteins from panel F. Data are mean ± SEM (n = 8 per group, n. s. = no significance, *p < 0.05 compared to nondiabetic control; #p < 0.05 compared to T1DM).

glomerulosclerosis, glomerular vascular tufts, and interstitial expansion (Fig. 1E). Administration of KPF to diabetic mice normalized these diabetes-associated tubulo-glomerular histopathological changes (Fig. 1E). We then stained the kidney tissues with Sirius red and Masson Trichrome to assess fibrotic changes. Our results show increased collagen deposition in the interstitial compartment in diabetic mice, while KPF treatment reduced the levels of collagen deposition (Fig. 1E, Supplementary Fig.S2A-B). We supplemented these studies with qPCR analysis of collagen IV and transforming growth factor-β (TGF-β) and found increased transcript levels in kidney tissues from diabetic mice (Fig. 1F). In agreement with our histology findings showing reduced renal fibrosis upon KPF treatment, we show that KPF normalized the levels of collagen IV and TGF-β in the diabetic mouse kidneys (Fig. 1F). These results were confirmed using Western blot analysis (Fig. 1G, Supplementary Fig.S2C-D).

3.2. Kaempferol attenuates diabetes-induced inflammatory responses in kidneys

To assess whether the effects of KPF on preserving renal function and reducing fibrosis in diabetes are mediated through the modulation of inflammatory responses, we measured TNF-α and IL-6 levels. These proinflammatory factors are also involved in the TLR4-TRAF6-NF-κB pathway (Jialal et al., 2014). Immunohistochemical staining of kidney specimens from diabetic mice showed increased TNF-α immunoreactivity compared to non-diabetic controls (Fig. 2A, Supplementary Fig. S3). Such increase was not observed in diabetic mice treated with KPF. Treatment with KPF also significantly reduced TNF-α and IL-6 protein levels in diabetic mice as measured by ELISA (Fig. 2B–C).

We next assessed whether TLR4-TRAF6-NF-κB was involved in the actions of KPF. We know from previous studies that hyperglycemia-induced activation of TLR4-TRAF6-NF-κB signaling causes renal inflammation (Liu et al., 2014). Western blot analysis of IκBα showed decreased levels in kidney tissues of diabetic mice and preserved levels in mice treated with KPF (Fig. 2D–E). This readout signifies reversal of increased NF-κB activity in diabetic mice upon KPF treatment. We next examined the levels of TLR4, MyD88, and TRAF6 in mouse kidneys. Western blot analysis showed increased levels of TLR4, MyD88, and TRAF6 in kidneys from diabetic mice (Fig. 2F–I). Interestingly, we found that treatment of diabetic mice with KPF decreased the levels of TRAF6 without any alteration of TLR4 or MyD88 levels (Fig. 2F–I). These results suggest that KPF reduces NF-κB activation and inflammatory responses possibly by downregulating TRAF6.

3.3. TRAF6 deficiency prevents diabetes-induced renal dysfunction and fibrosis

To confirm the role of TRAF6 in renal inflammation and fibrosis in diabetes, we silenced TRAF6 using AAV2/2-shTRAF6. AAV2/2 has been reported to target kidney tissues for transgene expression (Qi et al., 2013). We injected AAV2/2-shTRAF6 through the tail vein, two weeks prior to STZ injection in male C57BL/6J mice. We confirmed the knockdown by Western blotting (Fig. 3A). Importantly, we show that knockdown of TRAF6 normalized STZ-induced kidney to body weight ratios, and levels of BUN, serum urinary albumin and creatine (Fig. 3B–E). It is interesting to note that knockdown of TRAF6 did not alter blood glucose levels and body weight profiles in diabetic mice (Supplementary Fig.S4A-B). These results indicate that the effects of KPF on blood glucose levels and body weights may be independent of TRAF6. Knockdown of TRAF6 was able to normalize morphological alterations in tubular epithelia, glomerulosclerosis, glomerular vascular tufts, and interstitial expansion in diabetic mouse kidneys (Fig. 3F). Sirius red and Masson staining also showed reduced collagen deposition and fibrosis upon knockdown of TRAF6 in diabetic mice (Fig. 3F, Supplementary Fig. S5A-B). Furthermore, silencing TRAF6 reduced both the mRNA and protein levels of collagen IV and TGF-β1 in diabetic mouse kidneys (Fig. 3G-H, Supplementary Fig.S5C-D).

3.4. Knockdown of TRAF6 reduces diabetes-induced inflammation in kidneys

To confirm the role of TRAF6 in diabetes-associated renal inflammation, we investigated the levels of proinflammatory factors in kidney tissues. Knockdown of TRAF6 showed reduced levels of TNF-α immunoreactivity (Fig. 4A, Supplementary Fig.S6A), and normalized levels of TNF-α and IL-6 transcripts in kidney tissues of diabetic mice (Fig. 4B). TRAF6 deficiency also reversed STZ-induced IκBα degradation (Fig. 4C, Supplementary Fig.S6B). To bolster these findings, we examined the levels of c-Jun N-terminal kinases (JNK) and TGF-β-activated kinase 1 (TAK1), two downstream kinases in the TRAF6 pro-inflammatory pathway. As shown in Fig. 4D, TRAF6 knockdown reduced the levels of phosphorylated JNK and TAK1 in diabetic mouse kidneys (Fig. 4D, Supplementary Fig.S6C-D). These findings suggest that TRAF6 initiates inflammatory responses in kidneys of diabetic mice through the activation of NF-κB and upregulation of proinflammatory cytokines.

3.5. TRAF6 expression is upregulated in tubular epithelial cells in diabetes

We examined the levels and localization of TRAF6 in kidney tissues to identify the cellular source. TRAF6 levels were increased in the kidneys of diabetic mice as detected using Western blot and qPCR analysis (Fig. 5A–B). Immunofluorescence staining showed TRAF6 immunoreactivity in cells expressing aquaporin 1 (AQP-1), implicating renal tubular epithelial cells as the cellular source/target (Fig. 5C). TRAF6 immunoreactivity, although significantly less, was also observed in Wilms tumor 1 (WT-1)-positive podocytes and glomeruli cells (Fig. 5D). These results indicate that renal tubular epithelial cells are perhaps the major contributor to the inflammatory responses in diabetic nephropathy.

3.6. KPF inhibits high glucose-induced NF-κB activity by reducing TRAF6 in cultured renal tubular epithelial cells

To provide mechanistic insights into the role of TRAF6 in diabetes-induced kidney dysfunction, we challenged cultured rat tubular epithelial cell line (NRK-52E) with high levels of glucose. NRK-52E cells were pre-treated with 2.5 μM KPF for 1 h and then stimulated with HG (33 mM) for 2, 4, 6, 8, 12 h. KPF pretreatment reduced the levels of TRAF6 protein in HG-stimulated NRK-52E cells (Fig. 6A–B). Similarly, KPF pretreatment decreased TRAF6 mRNA levels in HG-induced NRK-52E cells (Fig. 6C). Also, we observed reduced activation of NF-κB by KPF as evident through decreased nuclear translocation of NF-κB p65 subunit and degradation of IκBα in HG-stimulated NRK-52E cells (Fig. 6D, Supplementary Fig.S7). Consistent with these findings, KPF reduced HG-induced mRNA levels of TNF-α, IL-6 (Fig. 6E) and Collagen IV and TGF-β (Fig. 6F). In summary, there findings indicate that KPF inhibited HG-induced inflammatory responses in renal tubular cells by reducing TRAF6.

3.7. TRAF6 regulates proinflammatory pathway activation by high glucose in tubular epithelial cells

To confirm the importance of TRAF6 in mediating HG-induced proinflammatory pathway activation, we silenced the expression of TRAF6 using siRNA. Transfection of NRK-52E cells with siRNA targeting TRAF6 led to decreased TRAF6 expression as expected (Fig. 7A, Supplementary Fig.S8A), and reduced HG-induced phosphorylation of JNK and TAK1 (Fig. 7B, Supplementary Fig.S8B-C), and activation of NF-κB (Fig. 7C, Supplementary Fig.S8D-E). Similarly, silencing TRAF6 decreased the levels of TNF-α ,IL-6, Collagen IV and TGF-β mRNA induced by HG (Fig. 7D-E). We then overexpressed TRAF6 using pXC-TRAF6 plasmid transfection (Fig. 7F, Supplementary Fig.S8F) and

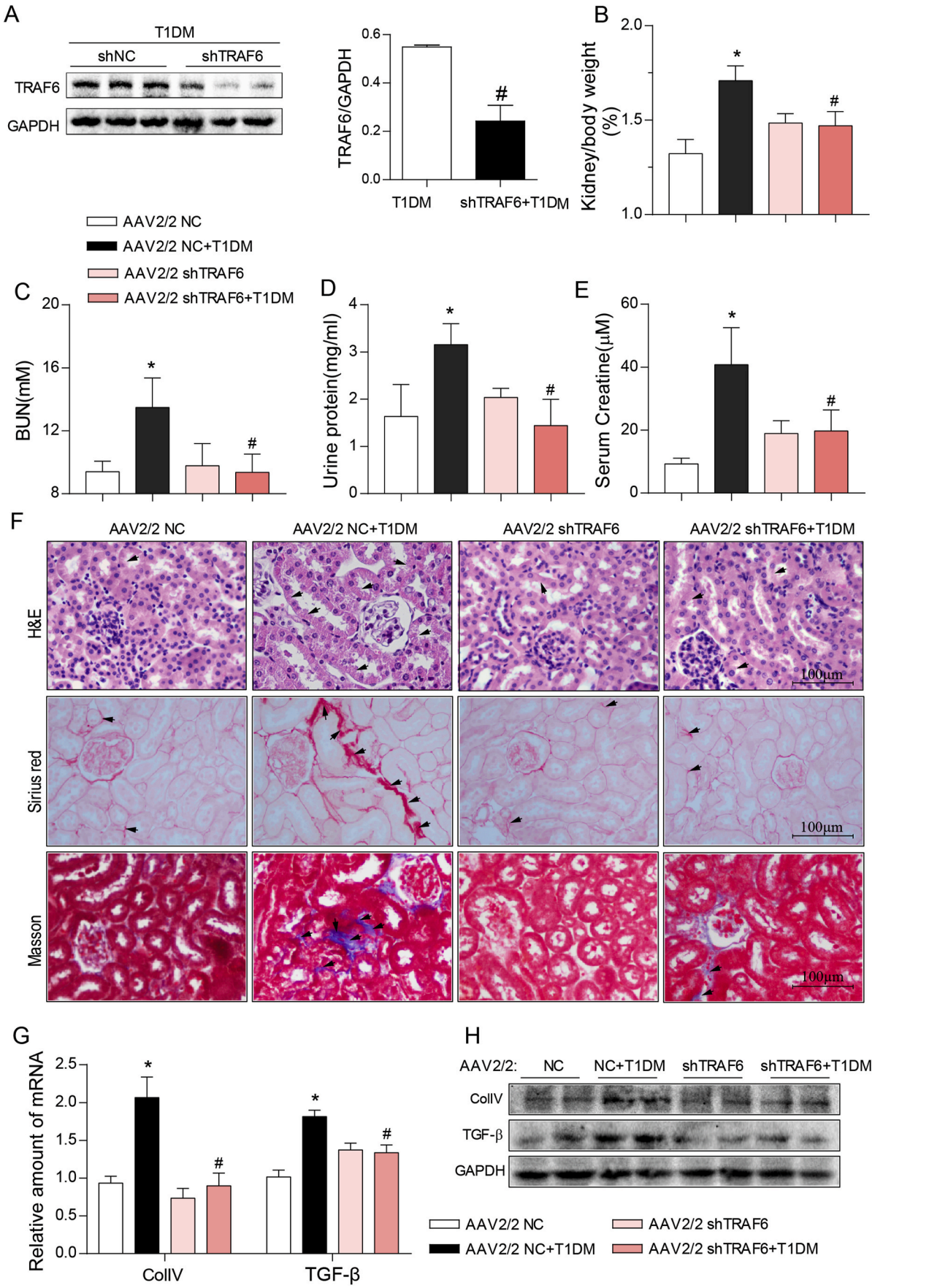

(caption on next page)

Fig. 3. Knocking down TRAF6 leads to preservation of kidney function in diabetes and normalization of tissue fibrosis. Diabetes was induced with STZ in male B6 mice. TRAF6 was knocked down by AAV2-shTRAF6 administered through tail vein injection. **(A)** Efficiency of TRAF6 knockdown following AAV2-shTRAF6 administration. Effects of TRAF6 silencing on kidney function were then evaluated by **(B)** assessing kidney to body weight ratios, and levels of **(C)** BUN, **(D)** serum Cr, and **(E)** urinary albumin. **(F)** Representative images of kidney tissues stained with H&E, Sirius red, and Masson Trichome [scale bar = 100 μm]. **(G)** Levels of Col-IV and TGF-β1 transcript levels in kidney tissues following silencing of TRAF6 [mRNA normalized to β-actin and reported relative to control]. **(H)** Representative blots showing levels of Col-IV, and TGF-β1. GAPDH was used as loading control. Data shown as mean ± SEM. n = 8 per group; *p < 0.05 compared to AAV2/2 NC; #p < 0.05 compared to AAV2/2 NC + T1DM. (For interpretation of the references to colour in this figure legend, the reader is referred to the Web version of this article.)

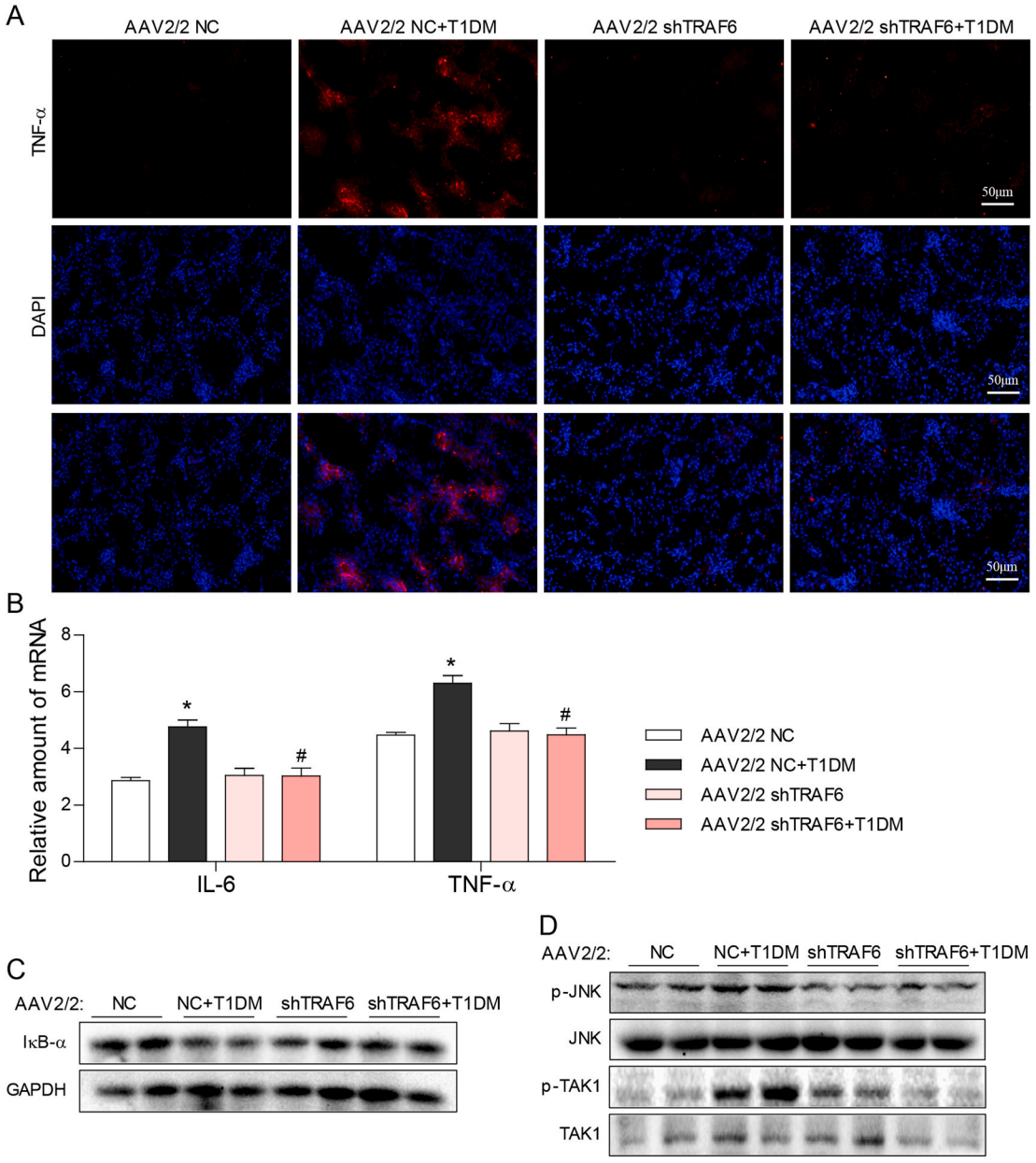

Fig. 4. Knockdown of TRAF6 attenuates diabetes-induced inflammatory pathway activation. (A) Representative images of TNF-α immunoreactivity in kidney tissues of mice following AAV2-shTRAF6 mediated TRAF6 silencing [scale bar = 50 μm]. **(B)** TNF-α and IL-6 mRNA levels in the kidney tissues as detected by qPCR [n = 8]. **(C)** Western blot analysis of IκB-α levels in kidney tissues. **(D)** Representative images for levels of phosphorylated and total JNK1/2 and TAK1 in kidney tissues [n = 8]. Data shown as mean ± SEM. n = 8 per group; *p < 0.05 compared to AAV2/2 NC; #p < 0.05 compared to AAV2/2 NC + T1DM.

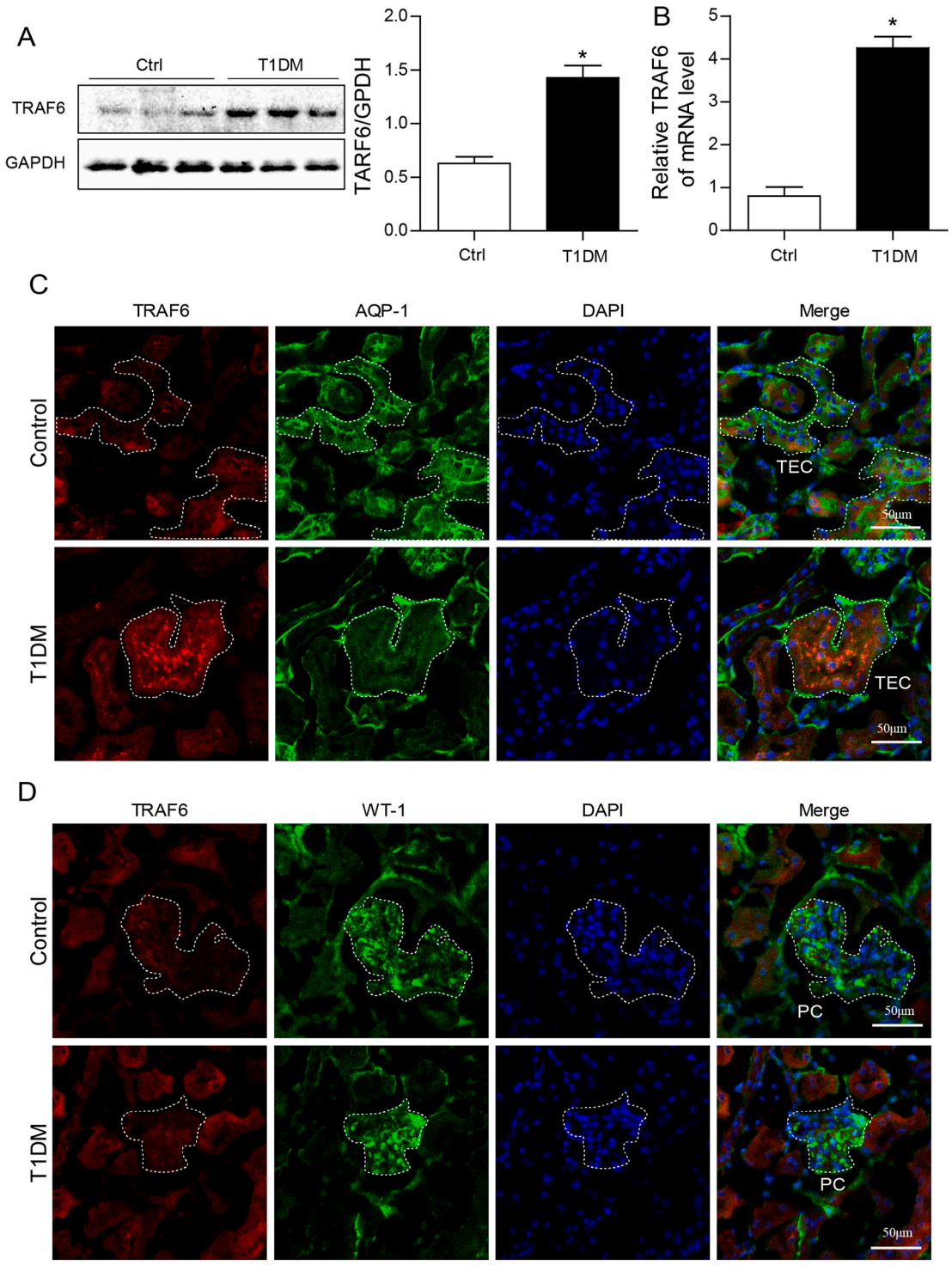

Fig. 5. TRAF6 expression is upregulated in kidney tissues in diabetes. (A) Western blot analysis and densitometric analysis of TRAF6 levels in kidney tissues from diabetic and nondiabetic control mice. **(B)** qPCR analysis of TRAF6 mRNA levels in kidney tissues [n = 6]. **(C)** Immunofluorescence staining of kidney tissues for TRAF6 (red) and aquaporin-1 (AQP-1, green). Aquaporin-1 was used as a marker of tubular epithelial cells (TEC). **(D)** Immunofluorescence staining for TRAF6 (red) and Wilms tumor 1 (WT-1, green) showing immunoreactivity of TRAF6 in podocytes (PC) [scale bar = 50 μm]. Merged images (yellow) showed co-localization as indicated by arrowheads. Data are mean ± SEM; n = 6 per group; *$p < 0.05$ compared to nondiabetic control. (For interpretation of the references to colour in this figure legend, the reader is referred to the Web version of this article.)

found activation of JNK1/2, TAK1, and NF-κB, and exacerbated responses to HG (Fig. 7G-H, Supplementary Fig.S8G-J). As expected, we found that TRAF6 overexpression caused further increases of mRNA levels of TNF-α, IL-6, Collagen IV and TGF-β upon HG stimulation (Fig. 7I-J). We also confirmed these findings in 293T cells without basic TRAF6 expression. TRAF6 expression in 293T cells via transfection with pXC-TRAF6 plasmid (Supplementary Fig.S9A) exacerbated HG-induced phosphorylation of JNK and TAK1, and activation of NF-κB (Supplementary Fig.S9B-C). This proinflammatory pathway activation was also reflected in increased TNF-α and IL-6 levels in 293T cells (Supplementary Fig.S9D-E).

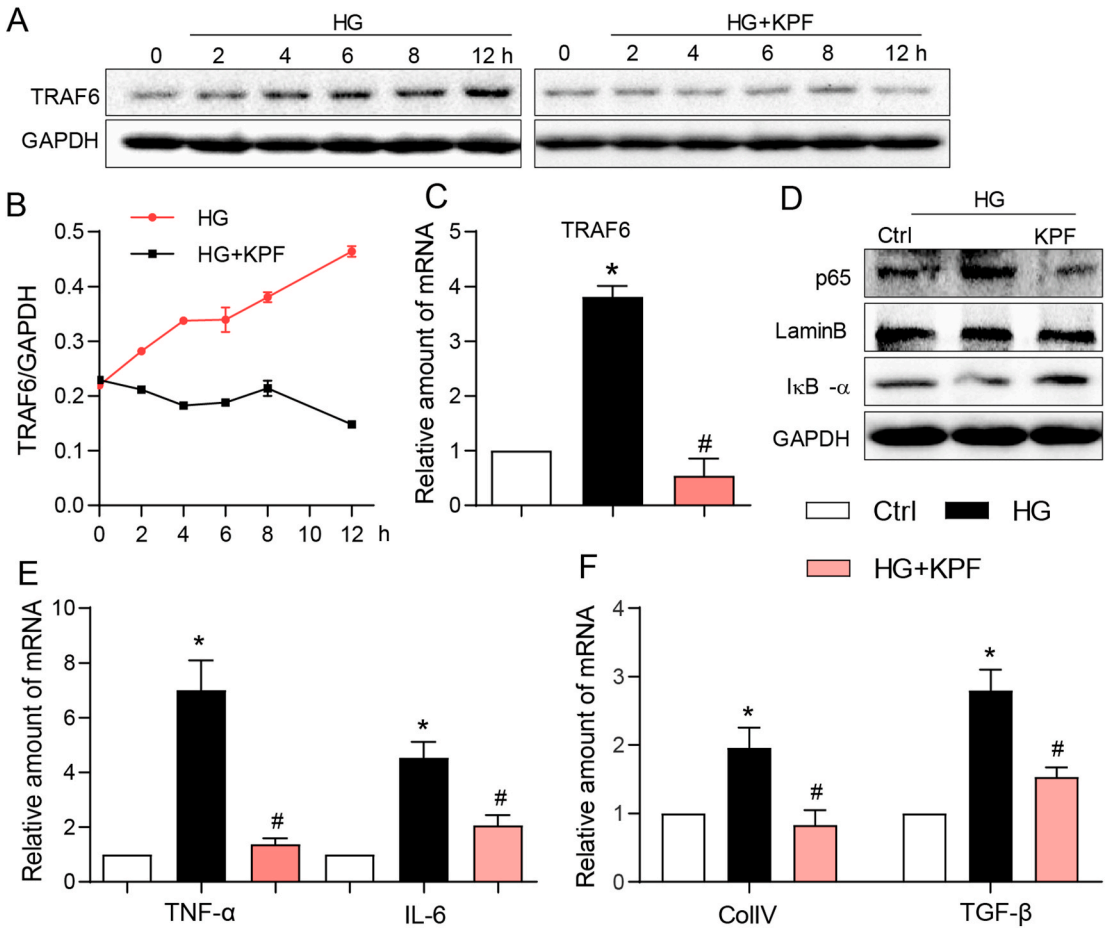

Fig. 6. Kaempferol inhibits HG-induced inflammatory factors by reducing TRAF6 in NRK-52E cells. (A) NRK-52E cells were pretreated with kaempferol at 2.5 μM for 1 h before exposure to high glucose (HG, 33 mM) for 2, 4, 6, 8, 12 h. Total proteins were extracted for Western blot analysis of TRAF6. **(B)** Densitometric quantification for panel A (means ± SEM, n = 5; *p < 0.05). **(C)** NRK-52E cells were pretreated with KPF for 1 h and then challenged with HG for 8 h. Figure showing levels of TRAF6 mRNA. **(D)** Cells were exposed to HG for 8 h, with or without pretreatment with KPF for 1 h, levels of nuclear NF-κB p65 and cytosolic IκB-α in cells were measured using Western blot. **(E–F)** The mRNA levels of proinflammatory cytokines (TNF-α and IL-6, E) and fibrosis genes (Col-IV and TGF-β, F) were detected in cells that have been exposed to HG for 12 h, with or without pretreatment with KPF for 1 h. Data shown as means ± SEM, n = 5 independent experiments, *p < 0.05 compared to control; #p < 0.05 compared to HG.

4. Discussion

It is well known that compounds with anti-oxidant and anti-inflammatory effects were potential candidates in the treatment of diabetic complications (Hamza et al., 2018). The salient finding of our study includes the demonstration that KPF protects against diabetes-associated inflammatory responses, fibrosis, and functional deficits in kidneys. We also show that these activities of KPF are, at least in part, mediated through the suppression of TRAF6. Analysis of kidney tissues shows upregulated levels of TRAF6 in tubular cells of diabetic mice. Knocking down the expression of TRAF6 in kidneys of diabetic mice or cultured renal tubular cells challenged with high levels of glucose, mirror the results obtained from KPF treatment. Finally, over-expression of TRAF6 in renal tubular cells aggravates inflammatory responses as evident by increased production of proinflammatory cytokines IL-6 and TNF-α. Collectively, our findings provide evidence that TRAF6 is a potential therapeutic target to normalize inflammation in DN, and KPF is a potential therapeutic agent for the treatment of DN.

Studies have shown that overactivation of TLR4-NF-κB inflammatory signaling leads to inflammation in kidneys and the progression of DN in experimental diabetes (Garibotto et al., 2017; T et al., 2016) and in T1DM patients (Dandona et al., 2013; S et al., 2013). Activation of NF-κB in hyperglycemia results in increased pro-inflammatory cytokine production (Lin et al., 2012) (Navarro-Gonzalez et al., 2011). Recent studies have also linked TRAF6 gene polymorphisms to diabetic vascular complications, including DN (Guo et al., 2016). Further implicating this pathway in DN are studies which show inhibition of inflammation upon TRAF6 deficiency (Liu et al., 2010; Kobayashi et al., 2003). TRAF6 uniquely participates in both TLR4 and TNFR signaling pathways. Therefore, it appears that TRAF6 may act as a central point of convergence where signals induced by TLR/TNFR families intersect. Consistent with our results, Zhou and coworkers reported an overexpression of TLR-4, MyD88, and TRAF6, and NF-κB activation in diabetic kidneys (Zhou et al., 2019). Interestingly, we found that KPF downregulated TRAF6 expression and inhibited NF-κB activation in the kidneys of diabetic mice but did not alter the levels of TLR4 and MyD88. These findings suggest that KPF might target TRAF6.

TRAF6 expression has been reported in dendritic cells (Kobayashi et al., 2003), and renal proximal tubule cells (Liu et al., 2010). We found that TRAF6 was upregulated in renal tubular epithelial cells in diabetic mice. Although studies are needed to examine the contribution of TRAF6 in other renal cells, we do show that suppression of TRAF6 in cultured renal tubular cells reduces NF-κB activity, and downstream expression of IL-6, TNF-α, as well as molecular markers of fibrosis. We also showed that TRAF6 overexpression intensified activation of NF-κB, and led to increased production of TNF-α and IL-6 in HG-induced NRK-52E cells. Elevated and sustained inflammation, including increased levels of proinflammatory cytokines IL-6 and TNF-α, is intricately linked to renal

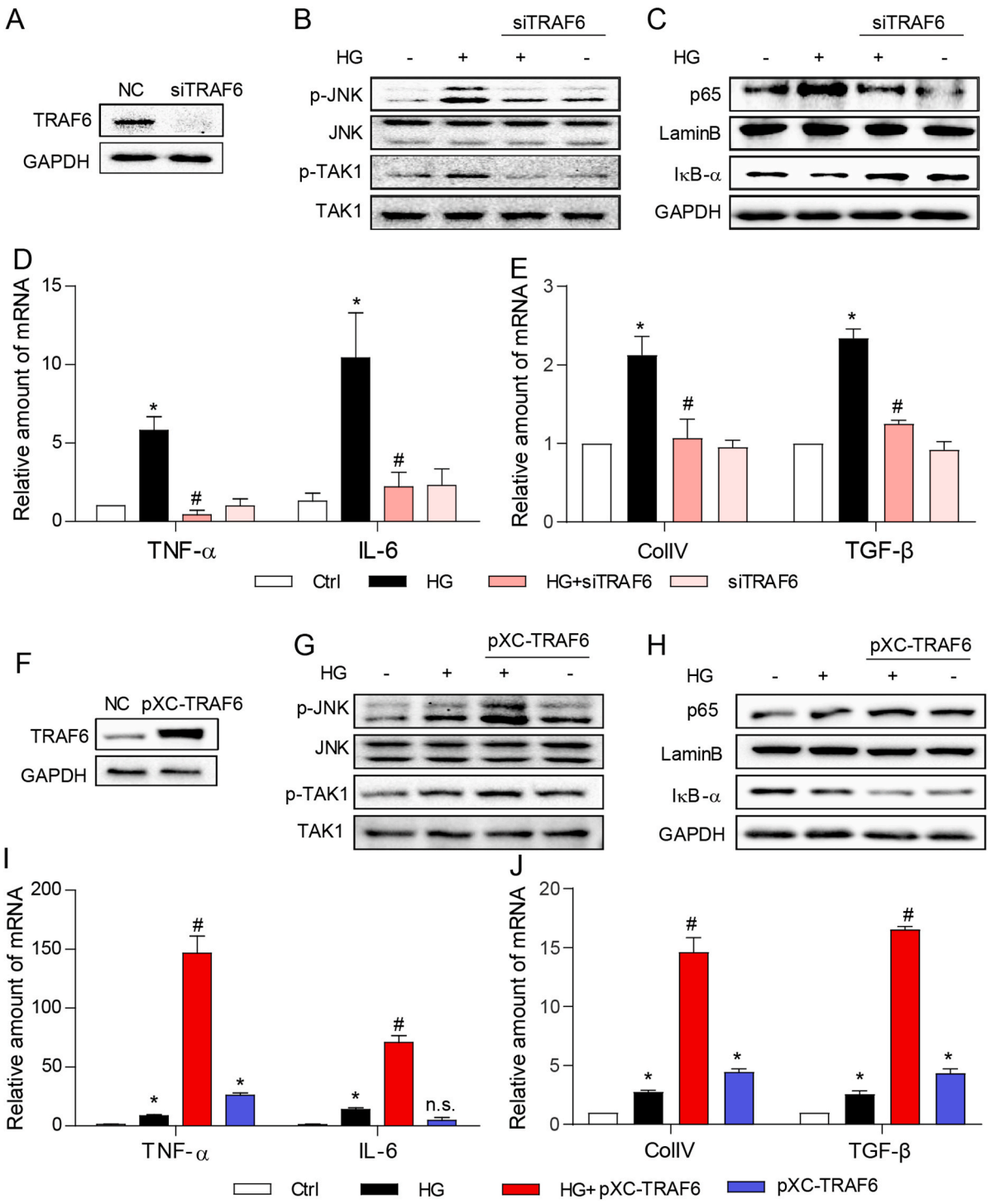

Fig. 7. TRAF6 overexpression exacerbates high glucose-induced inflammatory responses in renal cells. (A) NRK-52E cells were transfected with siRNA targeting TRAF6. Cells were then harvested and lysates were analyzed by Western blotting to measure TRAF6 levels. **(B)** TRAF6-silenced NRK-52E cells were stimulated with HG for 1 h. Phosphorylated and total protein levels of JNK1/2 and TAK1 were examined by Western blotting. **(C)** Levels of nuclear p65 and cytosolic IκB-α in TRAF6-silenced NRK-52E cells that have been exposed to HG for 8 h were measured by Western blot. Lamin B and GAPDH were used as the loading controls for nuclear and cytosolic proteins, respectively. **(D–E)** The mRNA levels of proinflammatory cytokines (TNF-α and IL-6, D) and fibrosis genes (Col-IV and TGF-β, E) in TRAF6-silenced NRK-52E cells that have been exposed to HG for 12 h were detected by qPCR. **(F)** TRAF6 was overexpressed in NRK-52E cells by infecting with harboring TRAF6 cDNA plasmid (pXC-TRAF6). Figure showing TRAF6 protein levels following overexpression. **(G)** Representative Western blots showing phosphorylated and total protein levels of JNK1/2 and TAK1 in TRAF6 overexpressed NRK-52E cells that have been exposed to HG for 1 h. **(H)** Levels of nuclear p65 and cytosolic IκB in TRAF6 overexpressed NRK-52E cells that have been exposed to HG for 8 h were detected by Western blot. Lamin B and GAPDH were used as the loading controls for nuclear and cytosolic proteins, respectively. **(I–J)** Proinflammatory cytokines (TNF-α and IL-6, I) and fibrosis genes (Col-IV and TGF-β, J) mRNA levels in NRK-52E cells following TRAF6 overexpressed plasmid transfection and exposed to HG for 12 h were detected by qPCR. Data shown as mean ± SEM; n = 5 independent experiments; n. s. = no significance; *p < 0.05 compared to control; #p < 0.05 compared to HG.

injuries (Aghadavod et al., 2016; Kobayashi et al., 2003). It is believed that increased IL-6 and TNF-α play a role in increased permeability, glomerular filtration rate, hemodynamic changes and renal hypertrophy (Baud and Ardaillou, 1995; ET et al., 1998; JF et al., 2006). In addition, inflammatory cytokines may also cause fibrosis by inducing the expression of collagens and fibrogenic factors such as TGF-β. Furthermore, increased collagen-IV and TGF-β regulate epithelial-mesenchymal transition (Wang et al., 2014). Recently, we found that inhibiting NF-κB activation results in decreased proinflammatory cytokine production and protects kidneys (Chen et al., 2018b). In the present study, we show that KPF reduced renal inflammation and fibrosis by downregulating TRAF6, which is upstream of NF-κB. These findings suggest that TRAF6 plays an important role in kidney inflammatory responses, and structural and functional characteristics of DN, and that TRAF6 blockade or pharmacological inhibition is protective against DN.

Another interesting finding of our study was that KPF impacted blood glucose levels (Supplementary Fig. S1), while TRAF6 knockdown did not. These findings suggest that KPF may have multiple targets. At least some of the effects of KPF may be related to its activities of scavenging free radicals and enhancing antioxidant potential (Liao et al., 2016). KPF has previously been shown to exhibit an anti-diabetic activity (Alkhalidy H. et al., 2018), including improvement of insulin signaling (Luo et al., 2015), protection of β-cells from glucose toxicity (Zhang and Liu, 2011). Collectively, our findings indicate that KPF potentially regulates inflammatory responses through TRAF6 and hyperglycemia possibly through off-target effects. However, the exact mechanism by which KPF downregulates TRAF6 expression remains to be investigated. Also, further studies are needed to reveal other beneficial functions of KPF.

5. Conclusion

In summary, our findings demonstrated that pharmacological inhibition of TRAF6 by KPF and knockdown of TRAF6 attenuate diabetes-associated renal inflammation, fibrosis and renal dysfunction. Our results reveal that TRAF6 expression is primarily localized to renal tubular epithelial cells, and inhibiting TRAF6 normalizes glucose-induced inflammatory factor expression by dampening NF-κB activation. Collectively, our studies provide evidence that TRAF6 plays a significant role in inflammatory responses in diabetic nephropathy. KPF, which exhibits a broad range of activity and low toxicity, make it an attractive chemical in the fight against various diseases. Both TRAF6 and KPF may represent interesting targets to combat diabetic nephropathy.

Author contributions

Wu Luo, Xiaojun Chen, Xuemei Chen, Xueting Hu, and Fei Zhuang: collection, analysis and interpretation of data; Jiangchang Qian, Yi Wang, Chao Zheng, and Guang Liang: conception and design, interpretation of data, manuscript writing, and manuscript revision.

Declaration of competing interest

The authors declare no conflict of interest.

Acknowledgements

We thank Prof. Zia Khan (Western University of Ontario, Canada) for language editing of the manuscript.

Financial support was provided by the National Key Research Project (2017YFA0506000), the National Natural Science Foundation of China (81872918, 81803600, and 81770825), and Natural Science Foundation of Zhejiang Province (LR18H160003, LY18H310011 and LR16H310001).

Appendix A. Supporting information

Supplemental data including 1 table and 9 figures can be found in the supplementary file. All the other data are available from the authors on request.

Appendix B. Supplementary data

Supplementary data to this article can be found online at https://doi.org/10.1016/j.jep.2020.113553.

References

Aghadavod, E., Khodadadi, S., Baradaran, A., Nasri, P., Bahmani, M., Rafieian-Kopaei, M., 2016. Role of oxidative stress and inflammatory factors in diabetic kidney disease. Iranian journal of kidney diseases 10, 337–343.

Akira, S., Takeda, K., 2004. Toll-like receptor signalling. Nat. Rev. Immunol. 4, 499–511.

Al-Dabbagh, B., Elhaty, I.A., Al Hrout, A., Al Sakkaf, R., El-Awady, R., Ashraf, S.S., Amin, A., 2018. Antioxidant and anticancer activities of Trigonella foenum-graecum, Cassia acutifolia and Rhazya stricta. BMC Compl. Alternative Med. 18, 240.

Al-Dabbagh, B., Elhaty, I.A., Elhaw, M., Murali, C., Al Mansoori, A., Awad, B., Amin, A., 2019. Antioxidant and anticancer activities of chamomile (Matricaria recutita L.). BMC Res. Notes 12, 3.

Alkhalidy, H., Moore, W., Wang, Y., Luo, J., McMillan, R.P., Zhen, W., Zhou, K., Liu, D., 2018. The flavonoid kaempferol ameliorates streptozotocin-induced diabetes by suppressing hepatic glucose production. Molecules 23.

S, T., K, A., Y, N., T, K., 2013. Pathophysiological mechanisms involving aggressive islet cell destruction in fulminant type 1 diabetes. Endocr. J. 60, 837–845.

O, K., J, N., Me, S., B, S., T, E., 2015. Kaempferol is an anti-inflammatory compound with activity towards NF-κB pathway proteins. Anticancer Res. 35, 2645–2650.

T, S., Cf, W., B, B., Kp, N., Rc, W., 2016. Toll-like receptor 4 activation contributes to diabetic bladder dysfunction in a murine model of type 1 diabetes. Diabetes 65, 3754–3764.

Baud, L., Ardaillou, R., 1995. Tumor necrosis factor in renal injury. Miner. Electrolyte Metab. 21, 336–341.

Chen, X., Qian, J., Wang, L., Li, J., Zhao, Y., Han, J., Khan, Z., Chen, X., Wang, J., Liang, G., 2018a. Kaempferol attenuates hyperglycemia-induced cardiac injuries by inhibiting inflammatory responses and oxidative stress. Endocrine 60, 83–94.

Chen, X., Yu, W., Li, W., Zhang, H., Huang, W., Wang, J., Zhu, W., Fang, Q., Chen, C., Li, X., Liang, G., 2018b. An anti-inflammatory chalcone derivative prevents heart and kidney from hyperlipidemia-induced injuries by attenuating inflammation. Toxicol. Appl. Pharmacol. 338, 43–53.

Dandona, P., Ghanim, H., Green, K., Sia, C.L., Abuaysheh, S., Kuhadiya, N., Batra, M., Dhindsa, S., Chaudhuri, A., 2013. Insulin infusion suppresses while glucose infusion induces Toll-like receptors and high-mobility group-B1 protein expression in mononuclear cells of type 1 diabetes patients. Am. J. Physiol. Endocrinol. Metab. 304, E810–E818.

Et, M., R, S., M, S., Jz, L., Xl, G., Kn, D., Vj, S., 1998. TNF-alpha increases albumin permeability of isolated rat glomeruli through the generation of superoxide. J. Am. Soc. Nephrol. : JASN (J. Am. Soc. Nephrol.) 9, 433–438.

Feng, H., Cao, J., Zhang, G., Wang, Y., 2017. Kaempferol attenuates cardiac hypertrophy via regulation of ASK1/MAPK signaling pathway and oxidative stress. Planta Med. 83, 837–845.

Garibotto, G., Carta, A., Picciotto, D., Viazzi, F., Verzola, D., 2017. Toll-like receptor-4 signaling mediates inflammation and tissue injury in diabetic nephropathy. J. Nephrol. 30, 719–727.

Gheith, O., Farouk, N., Nampoory, N., Halim, M.A., Al-Otaibi, T., 2016. Diabetic kidney disease: world wide difference of prevalence and risk factors. Journal of nephropharmacology 5, 49–56.

Guo, C., Zhang, L., Nie, L., Zhang, N., Xiao, D., Ye, X., Ou, M., Liu, Y., Zhang, B., Wang, M., Lin, H., Yang, G., Jing, C., 2016. Association of polymorphisms in the MyD88, IRAK4 and TRAF6 genes and susceptibility to type 2 diabetes mellitus and diabetic nephropathy in a southern Han Chinese population. Mol. Cell. Endocrinol. 429, 114–119.

Hamza, A.A., Fikry, E.M., Abdallah, W., Amin, A., 2018. Mechanistic insights into the augmented effect of bone marrow mesenchymal stem cells and thiazolidinediones in streptozotocin-nicotinamide induced diabetic rats. Sci. Rep. 8, 9827.

Jagadish, P.C., Latha, K.P., Mudgal, J., Nampurath, G.K., 2016. Extraction, characterization and evaluation of Kaempferia galanga L. (Zingiberaceae) rhizome extracts against acute and chronic inflammation in rats. J. Ethnopharmacol. 194, 434–439.

Jf, N., Fj, M., C, M., C, L., J, G., 2006. Renal pro-inflammatory cytokine gene expression in diabetic nephropathy: effect of angiotensin-converting enzyme inhibition and pentoxifylline administration. Am. J. Nephrol. 26, 562–570.

Jialal, I., Major, A.M., Devaraj, S., 2014. Global Toll-like receptor 4 knockout results in decreased renal inflammation, fibrosis and podocytopathy. J. Diabetes Complicat. 28, 755–761.

Kaur, H., Chien, A., Jialal, I., 2012. Hyperglycemia induces Toll like receptor 4 expression and activity in mouse mesangial cells: relevance to diabetic nephropathy. Am. J. Physiol. Ren. Physiol. 303, F1145–F1150.

Kim, T.W., Lee, S.Y., Kim, M., Cheon, C., Ko, S.G., 2018. Kaempferol induces autophagic cell death via IRE1-JNK-CHOP pathway and inhibition of G9a in gastric cancer cells. Cell Death Dis. 9, 875.

Kobayashi, T., Walsh, P.T., Walsh, M.C., Speirs, K.M., Chiffoleau, E., King, C.G., Hancock, W.W., Caamano, J.H., Hunter, C.A., Scott, P., Turka, L.A., Choi, Y., 2003. TRAF6 is a critical factor for dendritic cell maturation and development. Immunity 19, 353–363.

Kumar, A., 2020. Phytochemistry, pharmacological activities and uses of traditional medicinal plant Kaempferia galanga L. - an overview. J. Ethnopharmacol. 253, 112667.

Lenin, R., Sankaramoorthy, A., Mohan, V., Balasubramanyam, M., 2015. Altered immunometabolism at the interface of increased endoplasmic reticulum (ER) stress in patients with type 2 diabetes. J. Leukoc. Biol. 98, 615–622.

Liao, W., Chen, L., Ma, X., Jiao, R., Li, X., Wang, Y., 2016. Protective effects of kaempferol against reactive oxygen species-induced hemolysis and its antiproliferative activity on human cancer cells. Eur. J. Med. Chem. 114, 24–32.

Lim, A.K., Tesch, G.H., 2012. Inflammation in diabetic nephropathy. Mediat. Inflamm. 2012, 146154.

Lin, M., Yiu, W.H., Wu, H.J., Chan, L.Y., Leung, J.C., Au, W.S., Chan, K.W., Lai, K.N., Tang, S.C., 2012. Toll-like receptor 4 promotes tubular inflammation in diabetic nephropathy. J. Am. Soc. Nephrol. 23, 86–102.

Liu, S., Lutz, J., Chang, J., Liu, D., Heemann, U., Baumann, M., 2010. TRAF6 knockdown promotes survival and inhibits inflammatory response to lipopolysaccharides in rat primary renal proximal tubule cells. Acta Physiol. 199, 339–346.

Liu, P., Li, F., Qiu, M., He, L., 2014. Expression and cellular distribution of TLR4, MyD88, and NF-kappaB in diabetic renal tubulointerstitial fibrosis, in vitro and in vivo. Diabetes Res. Clin. Pract. 105, 206–216.

Luo, C., Yang, H., Tang, C., Yao, G., Kong, L., He, H., Zhou, Y., 2015. Kaempferol alleviates insulin resistance via hepatic IKK/NF-kappaB signal in type 2 diabetic rats. Int. Immunopharm. 28, 744–750.

Ma, J., Chadban, S.J., Zhao, C.Y., Chen, X., Kwan, T., Panchapakesan, U., Pollock, C.A., Wu, H., 2014. TLR4 activation promotes podocyte injury and interstitial fibrosis in diabetic nephropathy. PLoS One 9 e97985.

Navarro-Gonzalez, J.F., Mora-Fernandez, C., Muros de Fuentes, M., Garcia-Perez, J., 2011. Inflammatory molecules and pathways in the pathogenesis of diabetic nephropathy. Nat. Rev. Nephrol. 7, 327–340.

Qi, Y.F., Li, Q.H., Shenoy, V., Zingler, M., Jun, J.Y., Verma, A., Katovich, M.J., Raizada, M.K., 2013. Comparison of the transduction efficiency of tyrosine-mutant adeno-associated virus serotype vectors in kidney. Clin. Exp. Pharmacol. Physiol. 40, 53–55.

Reynolds, J.M., Martinez, G.J., Chung, Y., Dong, C., 2012. Toll-like receptor 4 signaling in T cells promotes autoimmune inflammation. Proc. Natl. Acad. Sci. U. S. A. 109, 13064–13069.

Varshney, R., Gupta, S., Roy, P., 2017. Cytoprotective effect of kaempferol against palmitic acid-induced pancreatic beta-cell death through modulation of autophagy via AMPK/mTOR signaling pathway. Mol. Cell. Endocrinol. 448, 1–20.

Wang, J.Y., Gao, Y.B., Zhang, N., Zou, D.W., Wang, P., Zhu, Z.Y., Li, J.Y., Zhou, S.N., Wang, S.C., Wang, Y.Y., Yang, J.K., 2014. miR-21 overexpression enhances TGF-beta1-induced epithelial-to-mesenchymal transition by target smad7 and aggravates renal damage in diabetic nephropathy. Mol. Cell. Endocrinol. 392, 163–172.

Xu, X.H., Zhao, C., Peng, Q., Xie, P., Liu, Q.H., 2017. Kaempferol inhibited VEGF and PGF expression and in vitro angiogenesis of HRECs under diabetic-like environment. Brazilian journal of medical and biological research = Revista brasileira de pesquisas medicas e biologicas 50 e5396.

Zang, Y., Zhang, L., Igarashi, K., Yu, C., 2015. The anti-obesity and anti-diabetic effects of kaempferol glycosides from unripe soybean leaves in high-fat-diet mice. Food Funct 6, 834–841.

Zhang, Y., Liu, D., 2011. Flavonol kaempferol improves chronic hyperglycemia-impaired pancreatic beta-cell viability and insulin secretory function. Eur. J. Pharmacol. 670, 325–332.

Zhou, B., Li, Q., Wang, J., Chen, P., Jiang, S., 2019. Ellagic acid attenuates streptozocin induced diabetic nephropathy via the regulation of oxidative stress and inflammatory signaling. Food Chem. Toxicol. 123, 16–27.